Transient Analysis of Single and Coupled Lines with Capacitively-Loaded Junctions

QIZHENG GU AND JIN AU KONG, FELLOW, IEEE

Abstract—**Transient processes are studied for a single line or a pair of coupled lines consisting of line sections with different characteristic admittances and with capacitances loaded at the junctions of line sections. Equations for the Laplace transform of the reflection and transmission coefficients of single and coupled lines are derived for the general case. When the capacitances are loaded at regular intervals, the corresponding expressions of the transient response waveforms at different terminal ports of these lines for both a step and a ramp input are developed. Based on the theoretical analysis, we illustrate the transient responses to ramp signals on some simplified computer signal lines, such as parallel-plate lines with transverse ridges, and parallel striplines with perpendicular crossing strips sandwiched between common upper and lower ground planes. The numerical results suggest that signals with a rise time of $t_r < 50$ ps will cause too much distortion, and should not be used when the length of the line is longer than 2 cm.**

I. Introduction

IN FIG. 1, WE illustrate an idealized and simplified model for signal transmission lines in a compact module of high-performance computers. As described in [1], the signal transmission lines are embedded in a dielectric and sandwiched between two conductive reference planes. Generally, these signal lines are separated into layers running in orthogonal directions. Signal lines in different layers are connected through vertical conductors called vias. The presence of the crossing strips and the vias causes the original signal lines to be loaded capacitively at certain intervals and the characteristic impedance of the signal lines to vary periodically. These effects give rise to crosstalk and distortion of signals propagating along the transmission line.

The transient analysis of transmission-line systems can be treated in the frequency domain in conjunction with transform techniques. Barnes [2] made use of the Fourier transform to analyze the impulse response of a uniformly coupled line system. Malaviya and Singh [3] investigated the propagation delay of an incident wave propagating along a uniform transmission line loaded capacitively at regular intervals. In terms of transform approaches, the propagation properties of a picosecond pulse on a dispersive transmission line [4] and the impulse response of a nonuniformly coupled line system [5] have been studied. The transient analysis of a passive microwave system has also been carried out directly in the time domain [6]–[11].

For the transmission-line configurations shown in Fig. 1, we shall use the expanded form of the reflection and transmission coefficients in these systems and their Laplace transforms to study the transient processes, generalizing the method used by Malaviya [3]. In the analysis, we assume that the transmission-line parameters, such as the characteristic admittance Y, propagation velocity v, and discontinuity capacitance C_d, etc., are independent of frequency over the frequency range of interest, and that influences between adjacent discontinuities are neglected.

Manuscript received November 5, 1985; revised April 27, 1986. This work was supported in part by the IBM Corporation, the Joint Services Electronics Programs, under Contract DAAG29-83-00038408, and in part by the Army Research Office under Contract DAAG29-85-K-0079.

The authors are with the Department of Electrical Engineering and Computer Science and the Research Laboratory of Electronics, Massachusetts Institute of Technology, Cambridge, MA 02139.

IEEE Log Number 8609605.

II. Transient Analysis for Capacitively-Loaded Lines

A generalized equivalent circuit of a single line with the configuration in Fig. 1 is depicted in Fig. 2, where Y_i $(i = 0,1,2,\cdots,n+1)$ are the characteristic admittances of different line sections, some of which result from the crossing strips or other perturbations. In Fig. 2, C_i $(i = 0,1,\cdots,n)$ are the equivalent lumped capacitances of discontinuities in the line, and l_i $(i = 0,1,2,\cdots,n+1)$ is the length of each line section.

The Laplace transform of the reflection coefficient Γ at the input port has the following form:

$$\begin{aligned}\Gamma(s) &= \frac{V_r(s)}{V_{\text{in}}(s)} \\ &= \Gamma_{01} + \sum_{m=1}^{n} \Gamma_{m,m+1} \prod_{k=0}^{m-1} (T_{k,k+1}T_{k+1,k}) \\ &\quad \cdot \exp\left(-2s \sum_{k=1}^{m} \tau_k\right) \\ &\quad \cdot \left\{1 + \sum_{i=0}^{m-1} \sum_{j=i+1}^{n} \Gamma_{i+1,i}\Gamma_{j,j+1} \right. \\ &\quad \cdot \prod_{k=i+1}^{j-1} (T_{k,k+1}T_{k+1,k}) \cdot \exp\left(-2s \sum_{k=i+1}^{j} \tau_k\right) \\ &\quad + \sum_{i=0}^{m-1} \sum_{j=i+1}^{n} \sum_{p=0}^{j-1} \sum_{q=p+1}^{n} \Gamma_{i+1,i}\Gamma_{j,j+1}\Gamma_{p+1,p}\Gamma_{q,q+1} \\ &\quad \cdot \prod_{k=i+1}^{j-1} (T_{k,k+1}T_{k+1,k}) \prod_{k=p+1}^{q-1} (T_{k,k+1}T_{k+1,k}) \\ &\quad \left. \cdot \exp\left[-2s\left(\sum_{k=i+1}^{j} \tau_k + \sum_{k=p+1}^{q} \tau_k\right)\right] + \cdots \right\} \end{aligned} \quad (1)$$

0018-9480/86/0900-0952$01.00 ©1986 IEEE

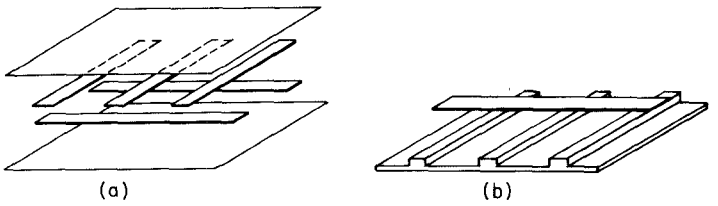

Fig. 1. Transmission-line configurations under consideration.

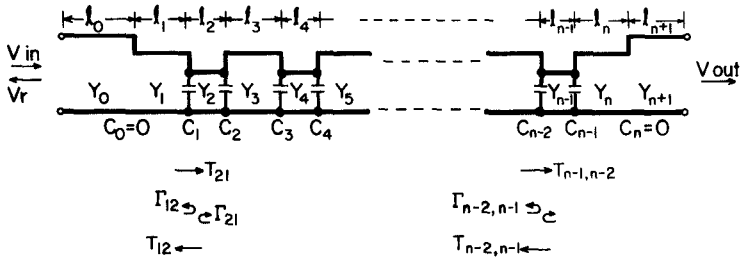

Fig. 2. A generalized equivalent circuit.

where

$$\Gamma_{i,i+1}=\frac{Y_i-sC_i-Y_{i+1}}{Y_i+sC_i+Y_{i+1}} \tag{2}$$

$$\Gamma_{i+1,i}=\frac{Y_{i+1}-sC_i-Y_i}{Y_i+sC_i+Y_{i+1}}=-\Gamma_{i,i+1}-2\gamma_i \tag{3}$$

$$\gamma_i=\frac{sC_i}{Y_i+sC_i+Y_{i+1}} \qquad \tau_i=\frac{l_i}{v_i} \tag{4}$$

$$T_{i+1,i}=1+\Gamma_{i,i+1}=\frac{2Y_i}{Y_i+sC_i+Y_{i+1}} \tag{5}$$

$$T_{i,i+1}=1+\Gamma_{i+1,i}=\frac{2Y_{i+1}}{Y_i+sC_i+Y_{i+1}} \tag{6}$$

and v_i is the signal propagation velocity on the ith line section. The double subscript $(i,i+1)$ denotes that the corresponding coefficient from the $(i+1)$th section to the ith. For instance, $\Gamma_{i,i+1}$ is the reflection coefficient for the signal reflected back into the ith section from the $(i,i+1)$ interface and $T_{i+1,i}$ is the transmission coefficient from the ith to the $(i+1)$th section. On the right-hand side of (1), Γ_{01} is the reflection coefficient at the first discontinuity, the single summation term includes all the contributions from the reflections at the other discontinuities in the line, and the multiple summation terms represent the contributions of undergoing multiple reflections coming out from the input port. Equation (1) contains only those contributions generated through an odd number of reflections. The exponential factors in this equation express the time delays of the different reflections appearing at the input port. We should also mention that the product series will be equal to 1 when the upper limit of it is less than the lower limit.

Similarly, the transmission coefficient $T(s)$ for the signal at the output port relative to that at the input port is

$$\begin{aligned}T(s)&=\frac{V_{\text{out}}(s)}{V_{\text{in}}(s)}\\&=\prod_{m=0}^{n}T_{m+1,m}\exp\left(-s\sum_{k=1}^{n}\tau_k\right)\\&\quad\cdot\left\{1+\sum_{i=1}^{n}\sum_{j=0}^{i-1}\Gamma_{i,i+1}\Gamma_{j+1,j}\right.\\&\quad\cdot\prod_{k=j+1}^{i-1}(T_{k,k+1}T_{k+1,k})\cdot\exp\left(-2s\sum_{k=j+1}^{i}\tau_k\right)\\&\quad+\sum_{i=1}^{n}\sum_{j=0}^{i-1}\sum_{p=j+1}^{n}\sum_{q=0}^{p-1}\Gamma_{i,i+1}\Gamma_{j+1,j}\Gamma_{p,p+1}\Gamma_{q+1,q}\\&\quad\cdot\prod_{k=j+1}^{i-1}(T_{k,k+1}T_{k+1,k})\prod_{k=q+1}^{p-1}(T_{k,k+1}T_{k+1,k})\\&\quad\left.\cdot\exp\left[-2s\left(\sum_{k=j+1}^{i}\tau_k+\sum_{k=q+1}^{p}\tau_k\right)\right]+\cdots\right\}\end{aligned} \tag{7}$$

where the parameters have the same meaning as those in (1). It comprises the contributions of the signals directly passing through the line and undergoing an even number of reflections between discontinuities before coming out from the output port.

In many practical situations, the above line configuration is a periodic structure consisting of two kinds of transmission-line sections and some capacitances loaded at regular intervals, where

$$\begin{aligned}&Y_0=Y_{n+1}\\&Y_1=Y_3=\cdots=Y_{2k+1} \qquad \left(k=1,2,3,\cdots,\frac{n-1}{2}\right)\\&l_1=l_3=\cdots=l_{2k+1}\\&Y_2=Y_4=\cdots=Y_{2k}\\&l_2=l_4=\cdots=l_{2k}\\&C_1=C_2=\cdots=C_i=\cdots=C_d.\end{aligned}$$

The reflection coefficient $\Gamma_{i,i+1}$ and the transmission coefficient $T_{i,i+1}$, therefore, can be simplified into the following forms:

$$\Gamma_{01} = -\Gamma_{10} = -\Gamma_{n+1,n} = \Gamma_{n,n+1} = \frac{Y_0 - Y_1}{Y_0 + Y_1} \tag{8}$$

$$\Gamma_{2k-1,2k} = \Gamma_{2k-1,2k-2} = \frac{Y_1 - Y_2 - sC_d}{Y_1 + Y_2 + sC_d} = -\frac{s + (-1)^{2k-1} a_2}{s + a_1} \tag{9}$$

$$\Gamma_{2k,2k-1} = \Gamma_{2k,2k+1} = \frac{Y_2 - Y_1 - sC_d}{Y_1 + Y_2 + sC_d} = -\frac{s + (-1)^{2k} a_2}{s + a_1} \tag{10}$$

$$T_{01} = T_{n,n+1} = \frac{2Y_0}{Y_0 + Y_1} \tag{11}$$

$$T_{10} = T_{n+1,n} = \frac{2Y_1}{Y_0 - Y_1} \tag{12}$$

$$T_{2k-1,2k} = T_{2k-1,2k-2} = \frac{2Y_2}{Y_1 + Y_2 + sC_d} = \frac{d_2}{s + a_1} \tag{13}$$

$$T_{2k,2k-1} = T_{2k,2k+1} = \frac{2Y_1}{Y_1 + Y_2 + sC_d} = \frac{d_1}{s + a_1} \tag{14}$$

where

$$a_1 = \frac{Y_1 + Y_2}{C_d} \quad a_2 = \frac{Y_1 - Y_2}{C_d}$$

$$d_j = \frac{2Y_j}{C_d} \qquad (j = 1,2). \tag{15}$$

In this case, using the inverse Laplace transform, we can obtain analytic expressions of the transient response waveforms for the reflection and transmission of some forms of signals. For a ramp signal with rise time t_r and amplitude V_{ino}, the reflected and transmitted signals have the following forms:

$$V_R(t) = \frac{V_{\text{ino}}}{t_r}\Bigg\{\Gamma_{01} t\,[U(t) - U(t - t_r)] - T_{01}T_{10} \cdot \Bigg[\Gamma_{01}\left(\frac{d}{a_1^2}\right)^{n-1} R_{tr}(2n-2, x_{[n/2]}) + \sum_{m=1}^{n-1}\left(\frac{d}{a_1^2}\right)^{m-1}\Bigg(R_{tr}(2m-2, x_{[m/2]}) - \frac{\Delta a_m}{a_1^2} R_{tr}(2m-1, x_{[m/2]})\Bigg) + \text{terms generated through odd number, } (2k+1) \geq 3, \text{ of reflections}\Bigg]\Bigg\} \tag{16}$$

and

$$V_T(t) = \frac{V_{\text{ino}}}{t_r} T_{01}T_{10}\Bigg\{\left(\frac{d}{a_1^2}\right)^{(n-1)/2} R_{tr}(n-1, x_{[n/2]'}) + \text{terms generated through even number, } 2k \geq 2, \text{ of reflections}\Bigg\} \tag{17}$$

where

$$d = d_1 d_2$$

$$R_{tr}(n,x) = \frac{1}{a_1}[xP(n,x) - x_r P(n,x_r)] - \frac{n}{a_1}[P(n+1,x) - P(n+1,x_r)]$$

$$x_{[n/2]} = a_1(t - 2\tau_{[n/2]})$$

$$x_{[n/2]'} = a_1(t - \tau_{[n/2]})$$

$$x_r = x - a_1 t_r$$

$$\tau_{[n/2]} = \left[\frac{n}{2}\right](\tau_1 + \tau_2) + \frac{1 - (-1)^n}{2}\tau_1.$$

$U(t)$ is the step function with an unit amplitude, $P(n,x)$ is the incomplete gamma function, and $[n/2]$ denotes the integer part of $n/2$. The detailed expressions of (16) and (17) and their derivations are given in Appendix A. The expressions for the transient response of the reflection and transmission of a step signal are also presented in the same appendix.

For the case of a pair of coupled lines capacitively-loaded as shown in Fig. 3, we can make use of the even- and odd-mode method and the Laplace transform to analyze their transient responses. In general, we may develop the equivalent circuits for the odd- and even-modes of the capacitively-loaded coupled lines as illustrated in Fig. 4.

Comparing Fig. 4 with Fig. 2, we find that they have similar configurations; hence, the formulas for single lines are still valid here except for corresponding changes in parameters, such as, admittances Y_i $(i = 1,2)$, and the discontinuity capacitances C_d are to be replaced by $Y_i^{\text{o,e}}$ and $C_{d\text{o,e}}$. Assuming the transient responses of the reflection and transmission in the odd- and even-mode circuits of Fig. 4 to be $V_R^{\text{o,e}}(t)$ and $V_T^{\text{o,e}}(t)$, we write the output waveforms from each terminal port in Fig. 3 as

$$V_1(t) = \tfrac{1}{2}[V_R^{\text{e}}(t) + V_R^{\text{o}}(t)] \tag{18}$$

$$V_2(t) = \tfrac{1}{2}[V_R^{\text{e}}(t) - V_R^{\text{o}}(t)] \tag{19}$$

$$V_3(t) = \tfrac{1}{2}[V_T^{\text{e}}(t) + V_T^{\text{o}}(t)] \tag{20}$$

and

$$V_4(t) = \tfrac{1}{2}[V_T^{\text{e}}(t) - V_T^{\text{o}}(t)] \tag{21}$$

where $V_R^{\text{o,e}}(t)$ and $V_T^{\text{o,e}}(t)$ are given by (16) and (17) (or (A15) and (A16)), with suitable parameters $Y_{i\text{o,e}}$ and $C_{d\text{o,e}}$ for a ramp input, or by (A6) and (A7) for a step input.

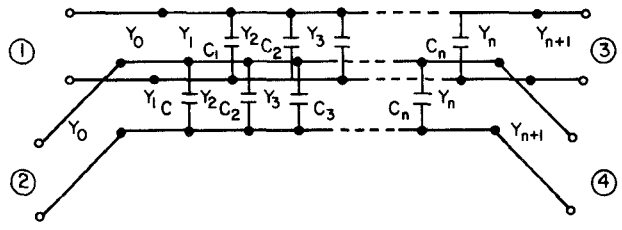

Fig. 3. Capacitively-loaded coupled transmission lines.

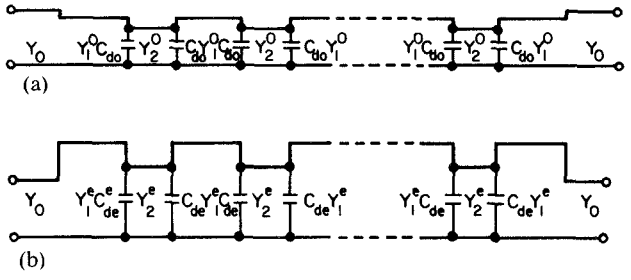

Fig. 4. Equivalent circuits for (a) the odd mode and (b) the even mode.

III. Analysis of a Parallel-Plate Transmission Line with Transverse Ridges

We now make use of the results and formulas presented in the above sections to deal with the transient response of a parallel-plate line with periodical transverse ridges as depicted in Fig. 5. We consider the equivalent circuit to consist of two kinds of lines with different characteristic admittances together with discontinuity capacitances at junctions. The equivalent circuit of this line configuration is shown in Fig. 6.

The capacitance per unit length of a parallel-plate transmission line with width w and height b is approximated as follows [13]:

$$\frac{1}{C_p} \simeq \frac{1}{\epsilon_r \epsilon_0}\left[\frac{K\left(\operatorname{sech}\frac{\pi w}{4b}\right)}{2K\left(\tanh\frac{\pi w}{4b}\right)} - \frac{b^2}{2\pi w^2}\ln\left(1+\frac{4w^2}{ab^2}\right)\right] \quad (22)$$

where K is the complete elliptic integral of the first kind, and $a = 2/\ln(4/\pi) = 8.2794$. Hence, the characteristic admittances Y_1 and Y_2 in Fig. 6 are

$$Y_i = \frac{\sqrt{\epsilon_r}}{60\pi}\frac{K(\tanh \pi w/4b_i)/K(\operatorname{sech}\pi w/4b_i)}{1-\dfrac{b_i^2}{\pi w^2}\dfrac{K(\tanh\pi w/4b_i)}{K(\operatorname{sech}\pi w/4b_i)}\ln\left(1+4w^2/ab_i^2\right)} \quad (i=1,2) \quad (23)$$

where

$$b_i = \begin{cases} b, & i=1 \\ b-d_0, & i=2. \end{cases} \quad (24)$$

The discontinuity capacitance C_d at the junction of two parallel-plate line sections with different admittances has

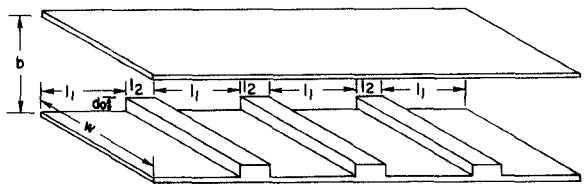

Fig. 5. A parallel-plate line with transverse ridges.

the following expression [14]:

$$C_d = \frac{\sqrt{\epsilon_r}bY_1}{\pi v_0}\left\{2\ln\frac{b^2-(b-d_0)^2}{4b(b-d_0)} + \left(\frac{b}{b-d_0}-\frac{b-d_0}{b}\right)\ln\frac{2b-d_0}{d_0} + \frac{2b^2}{\pi^2(b-d_0)^2}\sum_{n=1}^{\infty}\sin^2 n\pi\frac{b-d_0}{b}\cdot\left[\left(1-\frac{b^2w^2}{v_0^2n^2\pi^2}\right)^{-1/2}-1\right]\frac{1}{n^3}\right\}.$$

In our case, the maximum term ($n=1$) in the summation of the above equation is less than 1.6 percent of the first two terms on the right-hand side when the frequency is below 100 GHz. The higher order ($n \geqslant 2$) terms decay very rapidly because of the $1/n^3$ factor. The summation associated with the higher order modes can therefore be neglected. The discontinuity capacitance becomes frequency insensitive

$$C_d \cong \frac{\sqrt{\epsilon_r}bY_1}{\pi v_0}\left\{2\ln\frac{y(1-y)}{(1-2y)} + \left(\frac{1}{1-2y}+(1-2y)\right)\ln\frac{1-y}{y}\right\} \quad (25a)$$

where v_0 is the speed of light in free space, and

$$y = \frac{d_0}{2b}. \quad (25b)$$

The approximate expressions for the Laplace transform of the reflection and transmission coefficient take the form

$$\Gamma(s) = -\sum_{m=1}^{n-1}\frac{s+(-1)^m a_2}{s+a_1}\cdot\left(\frac{d}{(s+a_1)^2}\right)^{m-1}\exp\left(-2s\tau_{[m/2]}\right)\cdot\left\{1+\sum_{\substack{i=1\\ m\neq 1}}^{m-1}\sum_{j=i+1}^{n-1}\frac{\left(s+(-1)^{i+1}a_2\right)\left(s+(-1)^j a_2\right)}{(s+a_1)^2}\cdot\left(\frac{d}{(s+a_1)^2}\right)^{j-i-1}\exp\left(-2s\tau_{[(j-i)/2]}\right)\right\}.$$

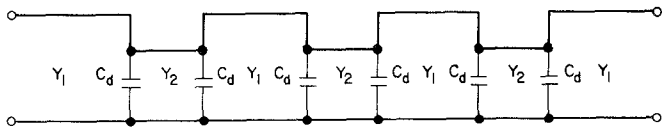

Fig. 6. Equivalent circuit of the line configuration in Fig. 5.

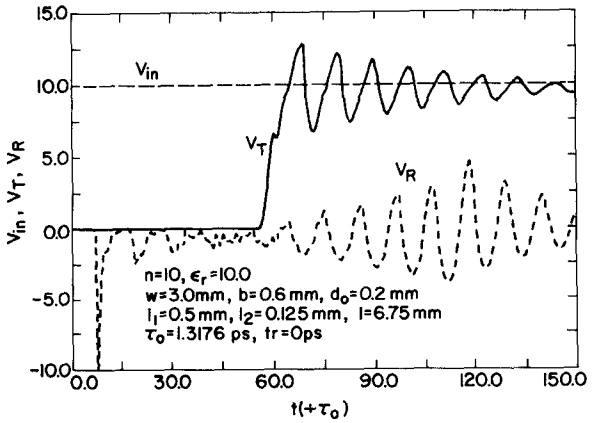

Fig. 7. The transient response for $n = 10$ to a step input.

and

$$T(s) = \left(\frac{d}{(s+a_1)^2}\right)^{(n-1)/2} \exp\left(-s\tau_{[m/2]}\right) \cdot \left\{1 + \sum_{i=2}^{n-1}\sum_{j=1}^{i=1} \frac{\left(s+(-1)^i a_2\right)\left(s+(-1)^{j+1}a_2\right)}{(s+a_1)^2} \cdot \left(\frac{d}{(s+a_1)^2}\right)^{i-j-1} \exp\left(-2s\tau_{[(i-j)/2]}\right)\right\}$$

These are the special cases of (A1) and (A2) in Appendix A. The corresponding time-domain waveforms for the step or ramp signal are given by (A6) and (A7) or (A15) and (A16), provided that $\Gamma_{01} = 0$ in those expressions.

Now we illustrate the transient processes on a parallel-plate of length $l = 5.375$ cm for $n = 10$ in Fig. 5. In the following calculations, we shall neglect the small changes of the lengths of the line sections due to the capacitive discontinuities. The remaining parameters are

$$w = 3.0 \text{ mm} \quad b = 0.6 \text{ mm} \quad d_0 = 0.2 \text{ mm}$$
$$l_1 = 0.5 \text{ mm} \quad l_2 = 0.125 \text{ mm} \quad \epsilon_r = 10.0.$$

When the line is terminated with the characteristic impedance of the corresponding parallel-plate line at both ends and the input signal is a step function with $V_{\text{ino}} = 10$, the waveforms of the reflected and transmitted signals on this line are as shown in Fig. 7. From this figure, we see that the waveform of the reflected signal has a very large negative pulse at the beginning, and subsequently oscillates. The large negative pulse is caused by the first capacitive discontinuity, and its amplitude equals $(-V_{\text{ino}})$. The maximum fluctuation range of the reflection waveform is from -3.935 to 4.615. The transmitted waveform also contains decaying oscillations. Its maximum and minimum values are 12.882 and 6.773, respectively.

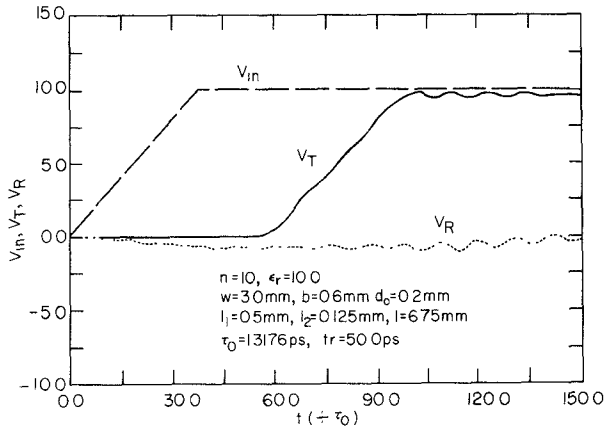

Fig. 8. The transient response to a ramp input with $t_r = 50$ ps.

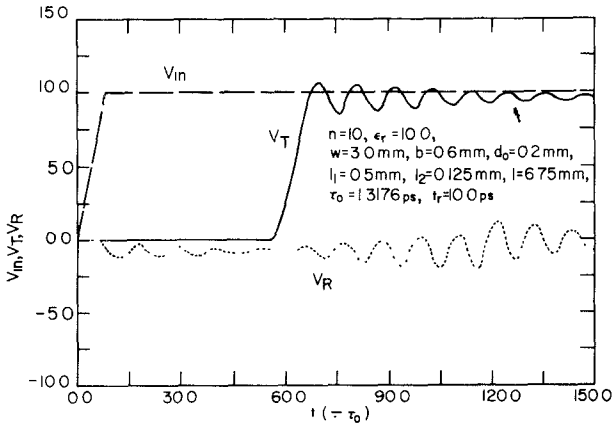

Fig. 9. The transient response to a ramp input with $t_r = 10$ ps.

When the input signal is a ramp function with a finite rise time t_r, the transient response for $t_r = 50$ ps and 10 ps are as presented in Figs. 8 and 9. For $t_r = 50$ ps, the maximum value of the reflected signal V_R is -1.030, and the rise time (measured at 90 percent of the signal amplitude) of the signal after it has passed through the line increased by approximately 2.3 ps. When the rise time becomes smaller, the waveform of the reflected signal increases rapidly in amplitude, and at the same time, the transmitted waveform deteriorates. For a smaller number of ridges with smaller ridge heights, both the reflected and transmitted waveforms will be improved.

IV. Analysis of Coupled Lines with Crossing Strips

For coupled lines with crossing strips, we employ the odd- and even-mode transmission lines as shown in Fig. 10. When there is no crossing strip, the odd- and even-mode admittances $Y_{1o,e}$ can be obtained from the corresponding capacitances $C_{1o,e}$ [12]. In this case, the phase velocities $v_{1o,e}$ of the odd- and even-mode are equal

$$v_{1o,e} = v_{10} = \frac{v_0}{\sqrt{\epsilon_r}}. \tag{26}$$

The crossing strips cause variation of the odd- and even-mode capacitance of the coupled lines. Their affect

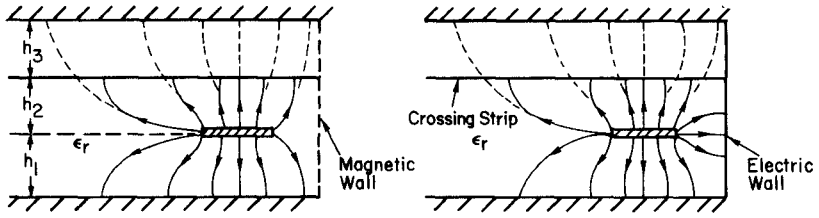

Fig. 10. The transverse sections of the even- and odd-mode transmission lines with crossing strip. —— Electric field line with crossing strip. ---- Electric field line without crossing strip. (a) Even mode. (b) Odd-mode.

on the corresponding odd- and even-mode inductance $L_{o,e}$ [1] is negligible. Hence, the characteristic admittance $Y_{1o,e}$ and the phase velocities $v_{2o,e}$ of the coupled-line section with the crossing strip can be related to those of the coupled-line section without the crossing strip as follows (see Appendix B):

$$Y_{2o,e} = a_{o,e} Y_{1o,e} \tag{27}$$

$$v_{2o,e} = v_{1o,e}/a_{o,e} \tag{28}$$

and

$$a_{o,e} = \sqrt{\frac{C_{2o,e}}{C_{1o,e}}}. \tag{29}$$

The discontinuity capacitances $C_{do,e}$ at the junctions of the two-line sections can be approximately estimated by means of (25) by modeling a stripline as a parallel-plate line with an effective width [15]. We use

$$Y_{1o,e} \cong \frac{\sqrt{\epsilon_r}(C_{1o,e} - C_{2o,e}/2)}{120\pi} \tag{30}$$

and

$$y_{o,e} = \frac{(h_2 + h_3) - d_0^{o,e}}{2(h_2 + h_3)} \tag{31}$$

$$d_0^{o,e} = \frac{2(C_{1o,e} - C_{2o,e}/2)(h_2 + h_3)}{C_{2o,e}} \tag{32}$$

When the formulas given in Section II are used to develop the transient response waveform at each port of the coupled lines, the following formulas should be taken into account:

$$a_{1o,e} = \frac{Y_{1o,e}(1 + a_{o,e})}{C_{do,e}}$$

$$a_{2o,e} = \frac{Y_{1o,e}(1 - a_{o,e})}{C_{do,e}}$$

$$d_{o,e} = \frac{4(Y_{1o,e})^2(1 - a_{o,e})}{C_{do,e}^2}$$

$$\tau^{o,e}_{[(i-j)/2]} = \left[\frac{i-j}{2}\right](\tau_1^{o,e} + \tau_2^{o,e}) + \frac{1-(-1)^{i-j}}{4} \cdot \left[\left(1-(-1)^{j+1}\right)\tau_1^{o,e} + \left(1+(-1)^{j+1}\right)\tau_2^{o,e}\right]$$

$$\tau_1^{o,e} = l_1/v_{1o,e} = \sqrt{\epsilon_r}\, l_1/v_0$$

$$\tau_2^{o,e} = l_2/v_{2o,e} = l_2 a_{o,e}/v_{1o,e}.$$

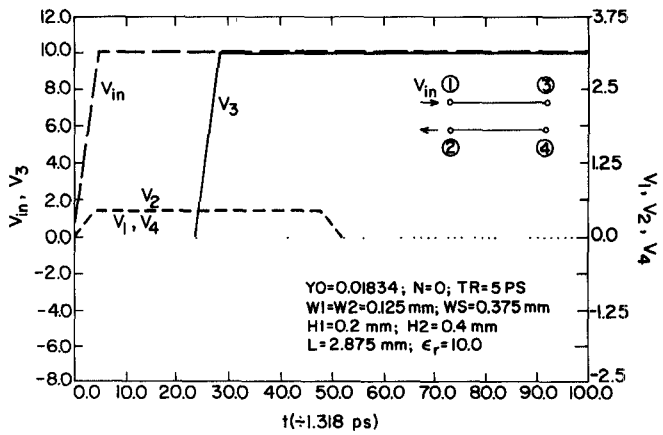

Fig. 11. The transient response at each port of coupled lines with matched terminals to a ramp input having $t_r = 5$ p.

We then employ the formulas (A15), (A16), and (18)–(21) to obtain the output transient waveform at each terminal port of the coupled lines with crossing strips.

Fig. 11 gives the transient responses of a pair of conventional coupled lines with matched terminals and the following parameters:

$$w_1 = w_2 = 0.125 \text{ mm} \quad w_s = 0.375 \text{ mm} \quad \epsilon_r = 10.0$$

$$h_1 = 0.2 \text{ mm} \quad h_2 + h_3 = 0.4 \text{ mm and } 1 = 2.875 \text{ mm}$$

where w_1 and w_2 are the widths of the transmission-line strips, w_s is the distance between the inside edges of two adjacent transmission line strips, ϵ_r is the relative permittivity of the medium filled in the lines, and l is the length of the coupled region. From this figure, we see that the unwanted output is the contra-directional coupling pulse V_2 at terminal port 2.

The presence of the crossing strips will obviously affect the transient processes of a digital signal traveling on a signal line as seen from the numerical results shown in Table I and Figs. 12–14. These results were obtained based on the calculation of a coupled-line system having the same configuration parameters as the foregoing except it is comprised of crossing strips suspended midway between transmission-line strips and the upper ground plate.

In Table I, we list our results and the data calculated according to (8) and the table in [1]. The table shows that the results from these two methods agree well. This confirms indirectly the validity of the various approximations used to estimate the capacitances. It should be emphasized

TABLE I
COMPARISON OF THE RESULTS AND THOSE FROM [1]

t_r (ps)	ℓ (mm)	Contra-directional Coupling: Average* Amplitude	Contra-directional Coupling: Reference [1] Eq 8(a) and Table 1	Co-directional Coupling: Pulse Avg * Amplitude	Co-directional Coupling: Reference [1] Eq 8(b) and Table 1
10	2.875	0 3080	0 2947	2 2948	invalid
50	2 875	0 3071	0.2947	1 3021	1 2750
100	2 875	0 3110	0 2947	0 6643	0 6373
500	2.875	0 3072	0.2947	0 1288	0 1275

* The average value is the mean of the amplitude in the plateau part of the waveform excluding the front and back edges In [1], eqn 8(a) is the average value of the near end noise, and eqn 8(b) is valid only when the difference in propagation delay along the coupled region of two modes is less than the rise time t_r.

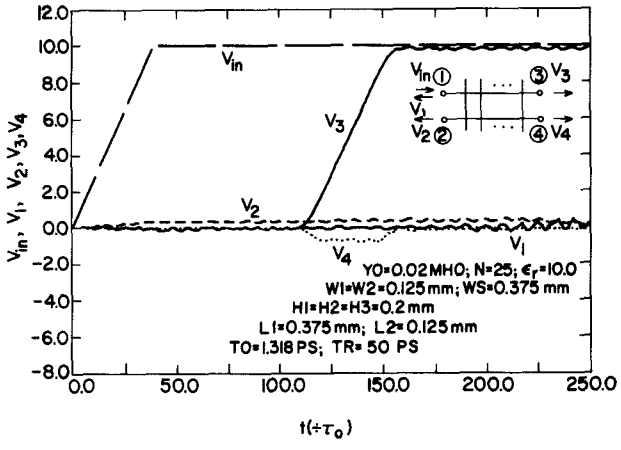

Fig. 12. The transient responses at each port of coupled lines with 25 crossing strips to a ramp input having $t_r = 50$ ps

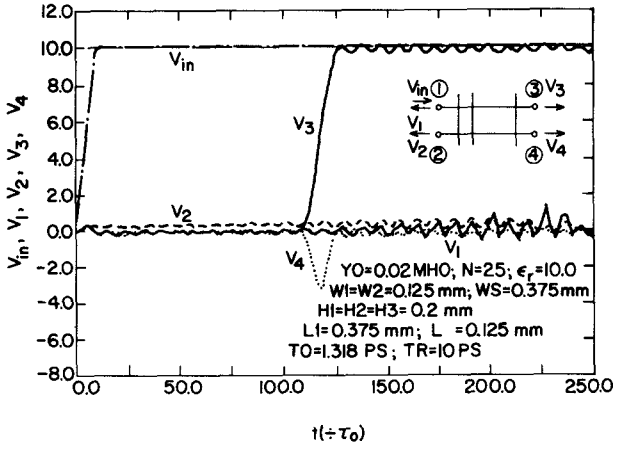

Fig. 13. The transient response at each p. crossing strips to a ramp input having $t_r = 10$ ps.

that this method can describe a transient process in detail, and is not restricted by the length of the coupled region and the rise time of signals as in [1].

When the length of l of the coupled region is extended and the corresponding number n of crossing strips is also increased, the unwanted signals, such as the reflection V_1, contra-directional coupling V_2, and co-directional coupling V_4, will obviously increase. As is evident from Fig. 14,

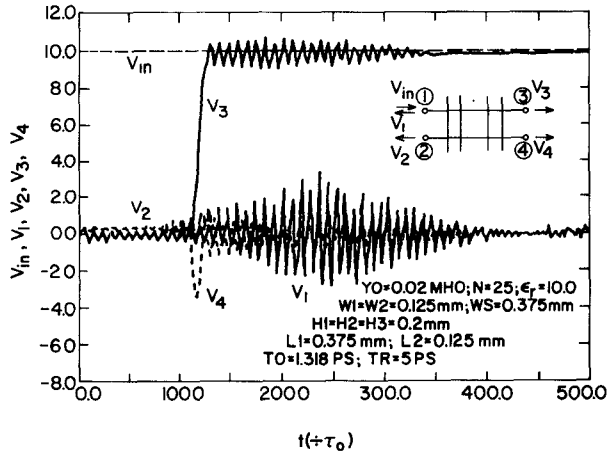

Fig. 14 The transient responses at each port of coupled lines with 25 crossing strips to a ramp input having $t_r = 5$ ps.

when l and n are increased, the reflection and contra-directional coupling waveform will exhibit strong oscillations. The amplitude of the co-directional coupling pulse not only depends on the rise time of the signals but also on the length of the coupled region. For instance, when the same ramp signal with rise time 10 ps passes through lines having length equal to 12.875 mm and 25.375 mm, the corresponding amplitudes of the V_4 pulse are, respectively, -3.14 and -5.49. It leads us to conclude that, for the present compact package, the above line configurations cannot be reliably used to propagate signals with rise time shorter than about 50 ps over a distance of 10 mm or more.

V. CONCLUSIONS

The method developed here can be successfully applied to the analysis of the transient process in a single transmission line capacitively-loaded at regular intervals and in coupled lines with capacitive obstacles. The obvious advantage of this method is that it enables us to obtain many important features of the transient process in the line system, without solving the cumbersome differential equations directly. Utilizing this method, we have analyzed two simplified models of signal transmission in a compact module of high-performance computers. The results of the analysis point out that the presence of the crossing strips in the multi-layer packaging configuration will cause serious reflections of the propagating signal on the original signal line, and a considerable co-directional and contra-directional coupling on the nearby lines when the rise time of the propagating signal decreases and/or the length of the signal line increases. Based on these, we are able to estimate the limit to the rise time of the signals propagating in the line. Although in the analysis we assume that the characteristic parameters are frequency-independent, the results are still-reliable because the dispersion effects are certainly of secondary importance over the frequency range of interest.

APPENDIX A
DERIVATION OF THE TRANSIENT RESPONSE EXPRESSIONS FOR THE PERIODIC STRUCTURE LOADED CAPACITIVELY

When conditions (8) are satisfied, the circuit of Fig. 2 becomes a periodic structure with loaded capacitances. Substituting (9)–(15) into (1) and (7), respectively, we obtain

$$\Gamma(s)=\Gamma_{01}+\sum_{m=1}^{n}\Gamma_{m,m+1}\left(\frac{d}{(s+a_1)^2}\right)^{m-1}T_{01}T_{10}\exp\left(-2s\tau_{[m/2]}\right)\Bigg\{1+\Gamma_{01}^2\left(\frac{d}{(s+a_1)^2}\right)^{n-1}\exp\left(-2s\tau_{[n/2]}\right)$$
$$+\Gamma_{01}\sum_{j=1}^{n-1}\frac{s+(-1)^j a_2}{s+a_1}\left(\frac{d}{(s+a_1)^2}\right)^{j-1}\exp\left(-2s\tau_{[j/2]}\right)+\Gamma_{01}\sum_{i=1}^{m-1}\frac{s+(-1)^{i+1}a_2}{s+a_1}\left(\frac{d}{(s+a_1)^2}\right)^{n-i-1}$$
$$\cdot\exp\left(-2s\tau_{[(n-i)/2]}\right)+\sum_{i=1}^{m-1}\sum_{j=i+1}^{n-1}\frac{\left(s+(-1)^{i+1}a_2\right)\left(s+(-1)^j a_2\right)}{(s+a_1)^2}$$
$$\cdot\left(\frac{d}{(s+a_1)^2}\right)^{j-i-1}\exp\left(-2s\tau_{[(j-i)/2]}\right)+\cdots\Bigg\} \tag{A1}$$

and

$$T(s)=T_{10}T_{01}\left(\frac{d}{(s+a_1)^2}\right)^{(n-1)/2}\exp\left(-s\tau_{[n/2]}\right)\Bigg\{1+\Gamma_{01}^2\left(\frac{d}{(s+a_1)^2}\right)^{n-1}\exp\left(-2s\tau_{[n/2]}\right)$$
$$+\Gamma_{01}\sum_{j=1}^{n-1}\frac{s+(-1)^{j+1}a_2}{s+a_1}\left(\frac{d}{(s+a_1)^2}\right)^{n-j-1}\exp\left(-2s\tau_{[(n-j)/2]}\right)+\Gamma_{01}\sum_{i=1}^{n-1}\frac{s+(-1)^i a_2}{s+a_1}\left(\frac{d}{(s+a_1)^2}\right)^{i-1}$$
$$\cdot\exp\left(-2s\tau_{[i/2]}\right)+\sum_{i=2}^{n-1}\sum_{j=1}^{i-1}\frac{\left(s+(-1)^i a_2\right)\left(s+(-1)^{j+1}a_2\right)}{(s+a_1)^2}\left(\frac{d}{(s+a)^2}\right)^{i-j-1}\exp\left(-2s\tau_{[(i-j)/2]}\right)+\cdots\Bigg\} \tag{A2}$$

where

$$d=d_1d_2=\frac{4Y_1Y_2}{c_d^2} \tag{A3}$$

$$\tau_{[(i-j)/2]}=\left[\frac{i-j}{2}\right](\tau_1+\tau_2)+\frac{1-(-1)^{i-j}}{4}\left[\left(1-(-1)^{j+1}\right)\tau_1+\left(1+(-1)^{j+1}\right)\tau_2\right] \tag{A4}$$

$$\tau_{[(i-j)/2]+[(p-q)/2]}=\tau_{[(i-j)/2]}+\tau_{[(p-q)/2]} \tag{A5}$$

and $[i/2]$ means taking the integers part of $i/2$. The terms in (A1) will be zero if their upper limit $m-1$ of the summations are equal to or less than zero.

When the magnitudes of the reflection coefficients are not very large, sufficient accuracy is achieved using (A1) and (A2) with only those terms corresponding to one, two, and three reflections.

For a step function input

$$V_{\text{in}}=V_{\text{ino}}U(t)$$
$$U(t)=\begin{cases}1, & t\geqslant 0\\ 0, & \text{otherwise}\end{cases}$$

the transient response waveforms of the reflected and transmitted signals on the line have the following expressions, respectively:

$$V_R(t)=V_{\text{ino}}\Bigg\{\Gamma_{01}U(t)-T_{01}T_{10}\Bigg[\Gamma_{01}\left(\frac{d}{a_1^2}\right)^{n-1}P\left(2n-2,x_{[n/2]}\right)$$
$$+\sum_{m=1}^{n-1}\left(\frac{d}{a_1^2}\right)^{m-1}\left(P\left(2m-2,x_{[m/2]}\right)-\frac{\Delta a_m}{a_1}P\left(2m-1,x_{[m/2]}\right)\right)+\Gamma_{01}^3\left(\frac{d}{a_1^2}\right)^{2n-2}P\left(4n-4,x_{[n/2]}\right)$$

$$+\Gamma_{01}^2\sum_{j=1}^{n-1}\left(\frac{d}{a_1^2}\right)^{n+j-2}\left(P\left(2(n+j)-4,x_{[n/2]+[j/2]}\right)-\frac{\Delta a_j}{a_1}P\left(2(n+j)-3,x_{[n/2]+[j/2]}\right)\right)$$

$$+\Gamma_{01}^2\sum_{i=1}^{n-1}\left(\frac{d}{a_1^2}\right)^{2n-i-2}\left(P\left(2(2n-i)-4,x_{[n/2]+[(n-i)/2]}\right)-\frac{\Delta a_{i+1}}{a_1}P\left(2(2n-i)-3,x_{[(n-i)/2]+[n/2]}\right)\right)$$

$$+\Gamma_{01}\sum_{i=1}^{n-1}\sum_{j=i+1}^{n-1}\left(\frac{d}{a_1^2}\right)^{n+j-i-2}\left(P\left(2(n+j-i)-4,x_{[n/2]+[(j-i)/2]}\right)\right.$$

$$\left.-\frac{\Delta a_{i+1}+\Delta a_j}{a_1}P\left(2(n+j-i)-3,x_{[n/2]+[(j-i)/2]}\right)+\frac{\Delta a_{i+1}\Delta a_j}{a_1^2}P\left(2(n+j-i)-2,x_{[n/2]+[(j-i)/2]}\right)\right)$$

$$+\Gamma_{01}^2\sum_{m=1}^{n-1}\left(\frac{d}{a_1^2}\right)^{n+m-2}\left(P\left(2(n+m)-4,x_{[n/2]+[m/2]}\right)-\frac{\Delta a_m}{a_1}P\left(2(n+m-2)+1,x_{[m/2]+[n/2]}\right)\right)$$

$$+\Gamma_{01}\sum_{m=2}^{n-1}\sum_{i=1}^{m-1}\left(\frac{d}{a_1^2}\right)^{n+m-i-2}\left(P\left(2(n+m-i)-4,x_{[(n-i)/2]+[m/2]}\right)\right.$$

$$\left.-\frac{\Delta a_{i+1}+\Delta a_m}{a_1}P\left(2(n+m-i)-3,x_{[(n-i)/2]+[m/2]}\right)+\frac{\Delta a_{i+1}\Delta a_m}{a_1^2}P\left(2(n+m-i)-2,x_{[(n-i)/2]+[m/2]}\right)\right)$$

$$+\Gamma_{01}\sum_{m=1}^{n-1}\sum_{j=1}^{n-1}\left(\frac{d}{a_1^2}\right)^{m+j-2}\left(P\left(2(m+j)-4,x_{[j/2]+[m/2]}\right)\right.$$

$$\left.-\frac{\Delta a_j+\Delta a_m}{a_1}P\left(2(m+j)-3,x_{[j/2]+[m/2]}\right)+\frac{\Delta a_j\Delta a_m}{a_1}P\left(2(m+j)-2,x_{[j/2]+[m/2]}\right)\right)$$

$$+\sum_{m=2}^{n-1}\sum_{i=1}^{m-1}\sum_{j=i+1}^{n-1}\left(\frac{d}{a_1^2}\right)^{m+j-i-2}\left(P\left(2(m+j-i)-4,x_{[(j-i)/2]+[m/2]}\right)-\frac{\Delta a_m+\Delta a_j+\Delta a_{i+1}}{a_1}\right.$$

$$\cdot P\left(2(m+j-i)-3,x_{[(j-i)/2]+[m/2]}\right)+\frac{\Delta a_m\Delta a_{i+1}+\Delta a_m\Delta a_j+\Delta a_{i+1}\Delta a_j}{a_1^2}P\left(2(m+j-i)-2,x_{[(j-i)/2]+[m/2]}\right)$$

$$\left.\left.-\frac{\Delta a_m\Delta a_{i+1}\Delta a_j}{a_1^3}P\left(2(m+j-i)-1,x_{[(j-i)/2]+[m/2]}\right)\right)\right]\Bigg\} \tag{A6}$$

and

$$V_T(t)=V_{\text{inc}}T_{01}T_{10}\left\{\left(\frac{d}{a_1^2}\right)^{(n-1)/2}P\left(n-1,x_{[n/2]'}\right)+\Gamma_{01}\sum_{j=1}^{n-1}\left(\frac{d}{a_1^2}\right)^{[3(n-1)-2j]/2}\left(P\left(3n-2(j+1)-1,x_{[(n-j)/2]+[n/2]'}\right)\right.\right.$$

$$\left.-\frac{\Delta a_{j+1}}{a_1}P\left(3n-2(j+1),x_{[(n-j)/2]+[n/2]'}\right)\right)+\Gamma_{01}^2\left(\frac{d}{a_1^2}\right)^{3(n-1)/2}P\left(3(n-1),x_{[n/2]+[n/2]'}\right)$$

$$+\Gamma_{01}\sum_{i=1}^{n-1}\left(\frac{d}{a_1^2}\right)^{[n+2(i-1)-1]/2}\left(P\left(n+2(i-1)-1,x_{[i/2]+[n/2]'}\right)-\frac{\Delta a_i}{a_1}P\left(n+2(i-1),x_{[i/2]+[n/2]'}\right)\right)$$

$$+\sum_{i=2}^{n-1}\sum_{j=1}^{i-1}\left(\frac{d}{a_1^2}\right)^{[n+2(i-j-1)-1]/2}\left(P\left(n+2(i-j-1)-1,x_{[(i-j)/2]+[n/2]'}\right)\right.$$

$$\left.-\frac{\Delta a_i+\Delta a_{j+1}}{a_1}P\left(n+2(i-j-1),x_{[(i-j)/2]+[n/2]'}\right)\right.$$

$$\left.\left.+\frac{\Delta a_i\Delta a_{j+1}}{a_1^2}P\left(n+2(i-j-1)+1,x_{[(i-j)/2]+[n/2]'}\right)\right)\right\} \tag{A7}$$

where $P(n, x)$ is the incomplete gamma function

$$P(n,x)=\frac{1}{(n-1)!}\int_0^x t^{n-1}e^{-t}\,dt=1-e^{-x}\sum_{k=0}^{n-1}\frac{x^k}{k!} \tag{A8}$$

$$P(0,x)=1 \tag{A9}$$

$$x_{[(i-j)/2]}=a_1\left(t-2\tau_{[(i-j)/2]}\right) \tag{A10}$$

$$x_{[n/2]'}=a_1\left(t-\tau_{[n/2]}\right) \tag{A11}$$

$$x_{[i/2]+[m/2]}=a_1\left[t-2\left(\tau_{[i/2]}+\tau_{[m/2]}\right)\right] \tag{A12}$$

$$x_{[(i-j)/2]+[n/2]'}=a_1\left[t-\left(2\tau_{[(i-j)/2]}+\tau_{[n/2]}\right)\right] \tag{A13}$$

and

$$\Delta a_i=a_1-(-1)^i a_2. \tag{A14}$$

For the case of a ramp input

$$V_{\text{in}}(t)=\frac{V_{\text{ino}}}{t_r}\left[tU(t)-(t-t_r)U(t-t_r)\right]$$

where $U(t)$ is a step function, and t_r is the rise time of the ramp step input. The corresponding transient responses for the reflected and transmitted signals of a capacitively-loaded transmission line will have similar forms to (A6) and (A7), except that the step function and the incomplete gamma function $P(n, s)$ are replaced by the ramp function and a function $R_{tr}(n, x)$, respectively, as follows:

$$\begin{aligned}
V_R(t)=V_{\text{ino}}\Bigg\{&\frac{\Gamma_{01}}{t_r}\left[tU(t)-(t-t_r)U(t-t_r)\right]-\frac{T_{01}T_{10}}{t_r}\Bigg[\Gamma_{01}\left(\frac{d}{a_1^2}\right)^{n-1}R_{tr}\left(2n-2,x_{[n/2]}\right)\\
&+(\Gamma_{01})^3\left(\frac{d}{a_1^2}\right)^{2n-2}R_{tr}\left(4n-4,2x_{[n/2]}\right)+\sum_{m=1}^{n-1}\left(\frac{d}{a_1^2}\right)^{m-1}\left(R_{tr}\left(2m-2,x_{[m/2]}\right)-\frac{\Delta a_m}{a_1}R_{tr}\left(2m-1,x_{[m/2]}\right)\right)\\
&+(\Gamma_{01})^2\sum_{j=1}^{n-1}\left(\frac{d}{a_1^2}\right)^{n+j-2}\left(R_{tr}\left(2(n+j)-4,x_{[n/2]+[j/2]}\right)-\frac{\Delta a_j}{a_1}R_{tr}\left(2(n+j)-3,x_{[n/2]+[j/2]}\right)\right)\\
&+(\Gamma_{01})^2\sum_{i=1}^{n-1}\left(\frac{d}{a_1^2}\right)^{2n-i-2}\left(R_{tr}\left(2(2n-i)-4,x_{[n/2]+[(n-i)/2]}\right)-\frac{\Delta a_{i+1}}{a_1}R_{tr}\left(2(2n-i)-3,x_{[(n-i)/2]+[n/2]}\right)\right)\\
&+\Gamma_{01}\sum_{i=1}^{m-1}\sum_{j=i+1}^{n-1}\left(\frac{d}{a_1^2}\right)^{n+j-i-2}\left(R_{tr}\left(2(n+j-i)-4,x_{[n/2]+[(j-i)/2]}\right)\right.\\
&\left.-\frac{\Delta a_{i+1}+\Delta a_j}{a_1}R_{tr}\left(2(n+j-i)-3,x_{[n/2]+[(j-i)/2]}\right)+\frac{\Delta a_{i+1}\Delta a_j}{a_1^2}R_{tr}\left(2(n+j-i)-2,x_{[n/2]+[(j-i)/2]}\right)\right)\\
&+(\Gamma_{01})^2\sum_{m=1}^{n-1}\left(\frac{d}{a_1^2}\right)^{n+m-2}\left(R_{tr}\left(2(n+m)-4,x_{[(n+m)/2]+[m/2]}\right)-\frac{\Delta a_m}{a_1}R_{tr}\left(2(n+m)-3,x_{[m/2]+[n/2]}\right)\right)\\
&+\Gamma_{01}\sum_{m=2}^{n-1}\sum_{i=1}^{m-1}\left(\frac{d}{a_1^2}\right)^{n+m-i-2}\left(R_{tr}\left(2(n+m-i)-4,x_{[(n-i)/2]+[m/2]}\right)\right.\\
&\left.-\frac{\Delta a_{i+1}+\Delta a_m}{a_1}R_{tr}\left(2(n+m-i)-3,x_{[(n-i)/2]+[m/2]}\right)+\frac{\Delta a_{i+1}\Delta a_m}{a_1^2}R_{tr}\left(2(n+m-i)-2,x_{[(n-i)/2]+[m/2]}\right)\right)\\
&+\Gamma_{01}\sum_{m=1}^{n-1}\sum_{j=1}^{n-1}\left(\frac{d}{a_1^2}\right)^{m+j-2}\left(R_{tr}\left(2(m+j)-4,x_{[j/2]+[m/2]}\right)-\frac{\Delta a_j+\Delta a_m}{a_1}R_{tr}\left(2(m+j)-3,x_{[j/2]+[m/2]}\right)\right.
\end{aligned}$$

$$+\frac{\Delta a_j \Delta a_m}{a_1^2} R_{tr}\left(2(m+j)-2, x_{[j/2]+[m/2]}\right)\Bigg) + \sum_{m=2}^{n-1}\sum_{i=1}^{m-1}\sum_{j=i+1}^{n-1}\left(\frac{d}{a_1}\right)^{m+j-i-2}$$

$$\cdot\Bigg(R_{tr}\left(2(m+j-i)-4, x_{[(j-i)/2]+[m/2]}\right) - \frac{\Delta a_m + \Delta a_j + \Delta a_{i+1}}{a_1} R_{tr}\left(2(m+j-i)-3, x_{[(j-i)/2]+[m/2]}\right)$$

$$+\frac{\Delta a_m \Delta a_{i+1} + \Delta a_m \Delta a_j + \Delta a_{i+1}\Delta a_j}{a_1^2} R_{tr}\left(2(m+j-i)-2, x_{[(j-i)/2]+[m/2]}\right)$$

$$-\frac{\Delta a_m \Delta a_{i+1}\Delta a_j}{a_1^3} R_{tr}\left(2(m+j-i)-1, x_{[(j-i)/2]+[m/2]}\right)\Bigg]\Bigg\} \tag{A15}$$

and

$$V_T(t) = \frac{V_{\text{ino}}}{t_r} T_{10}T_{01}\Bigg\{\left(\frac{d}{a_1^2}\right)^{(n-1)/2} R_{tr}\left(n-1, x_{[n/2]'}\right) + (\Gamma_{01})^2\left(\frac{d}{a_1^2}\right)^{3(n-1)/2} R_{tr}\left(3(n-1), x_{[n/2]+[n/2]'}\right)$$

$$+\Gamma_{01}\sum_{j=1}^{n-1}\left(\frac{d}{a_1^2}\right)^{[3(n-1)-2j]/2}\Bigg(R_{tr}\left(3n-2(j+1)-1, x_{[(n-j)/2]+[n/2]'}\right)$$

$$-\frac{\Delta a_{j+1}}{a_1} R_{tr}\left(3n-2(j+1), x_{[(n-j)/2]+[n/2]'}\right)\Bigg) + \Gamma_{01}\sum_{i=1}^{n-1}\left(\frac{d}{a_1^2}\right)^{[n+2(i-1)-1]/2}\Bigg(R_{tr}\left(n+2(i-1)-1, x_{[i/2]+[n/2]'}\right)$$

$$-\frac{\Delta a_i}{a_1} R_{tr}\left(n+2(i-1), x_{[i/2]+[n/2]'}\right)\Bigg) + \sum_{i=2}^{n-1}\sum_{j=1}^{i-1}\left(\frac{d}{a_1^2}\right)^{[n+2(i-j-1)-1]/2}$$

$$\cdot\Bigg[R_{tr}\left(n+2(i-j-1)-1, x_{[(i-j)/2]+[n/2]'}\right) - \frac{\Delta a_i + \Delta a_{j+1}}{a_1} R_{tr}\left(n+2(i-j-1), x_{[(i-j)/2]+[n/2]'}\right)$$

$$+\frac{\Delta a_i \Delta a_{j+1}}{a_1^2} R_{tr}\left(n+2(i-j-1)+1, x_{[(i-j)/2]+[n/2]'}\right)\Bigg]\Bigg\} \tag{A16}$$

where

$$R_{tr}(n,x) = \frac{1}{a_1}\left(xP(n,x) - x_r P(n,x_r)\right) - \frac{n}{a_1}\left(P(n+1,x) - P(n+1,x_r)\right) \tag{A17}$$

and

$$R_{tr}(0,x) = \frac{x}{a_1} U\left(\frac{x}{a_1}\right) - \frac{x_r}{a_1} U\left(\frac{x_r}{a_1}\right) = tU(t) - (t-t_r)U(t-t_r) \tag{A18}$$

where

$$x_r = x - a_1 t_r. \tag{A19}$$

The formulas analyzing the transient responses of the periodic structure loaded capacitively are useful not only to signal lines, but also to coupled lines.

Appendix B
Approach of Determining the Equivalent Parameters of the Coupled Striplines with Crossing Strips

For a pair of ordinary TEM coupled lines with the configuration shown in Fig. 15, the self-capacitances C_{11} and C_{12} of each line in the coupled lines, and the mutual-capacitance C_{12} between two lines can be obtained [12]

$$C_{11} = C_{10}' + C_{10} + C_{12}$$
$$C_{22} = C_{20}' + C_{20} + C_{12}$$

where C_{i0} and C_{i0}' $(i=1,2)$ include the corresponding fringing capacitances.

Assuming $C_{11} = C_{22}$, the odd- and even-mode capacitances can be derived [16] from the capacitances C_{11} and C_{12}

$$C_{1o} = C_{11} + C_{12}$$
$$C_{1e} = C_{11} - C_{12}.$$

The odd- and even-mode characteristic admittances are

$$Y_{1o} = v_{1o}\cdot \epsilon_0 \epsilon_r C_{1o}$$
$$Y_{1e} = v_{1e}\epsilon_0 \epsilon_r C_{1e}$$

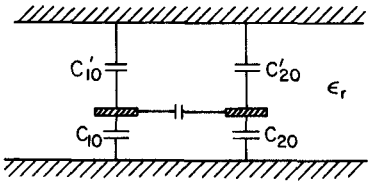

Fig. 15.

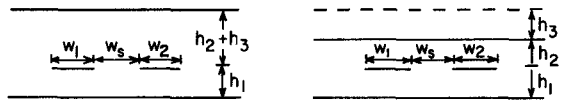

Fig. 16.

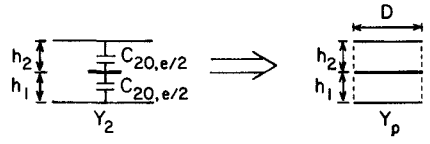

Fig. 17.

where ϵ_0 is the permittivity of the free space, and ϵ_r is the relative dielectric constant of the medium filled in the coupled lines.

Since the coupled lines are TEM mode lines, the phase velocities v_{1o} and v_{1e} of the odd- and even-mode are the same and equal to the velocity of the light in a homogeneous medium with a dielectric constant ϵ_r

$$v_{1o} = v_{1e} = \frac{v_0}{\sqrt{\epsilon_r}}.$$

The presence of crossing strips will only cause the variation of the odd- and even-mode capacitances of the coupled lines, it will not affect the corresponding odd- and even-mode inductances $L_{io,e}$ [1]. Using subscript 2 to denote the parameters associated with the line sections containing the crossing strips, we have

$$L_{1o} = L_{2o} \quad \text{and} \quad L_{1e} = L_{2e}. \tag{B1}$$

The odd- and even-mode capacitance C_{2o} and C_{2e} of the line sections with the crossing strips can be developed as before, but at present the upper ground plane is the crossing strip conductor instead of the original ground plane as illustrated in Fig. 16.

The phase velocities $v_{io,e}$ and the capacitances $C_{io,e}$ and inductances $L_{io,e}$ have the following relation:

$$v_{1o,e} = \frac{1}{\sqrt{\mu_0 L_{1o,e} \cdot \epsilon_0 \epsilon_r C_{1o,e}}}$$

and

$$v_{2o,e} = \frac{1}{\sqrt{\mu_0 L_{2o,e} \cdot \epsilon_0 \epsilon_r C_{2o,e}}}.$$

Making use of (B1), we obtain

$$a_{o,e} = \frac{v_{1o,e}}{v_{2o,e}} = \sqrt{\frac{C_{2o,e}}{C_{1o,e}}}$$

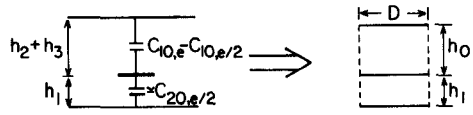

Fig. 18.

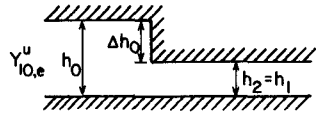

Fig. 19.

and

$$Y_{2o,e} = v_{2o,e} C_{2o,e} = a_{o,e} v_{10,e} C_{1o,e} = a_{o,e} Y_{1o,e}.$$

Now, we discuss the procedure for estimating the discontinuity capacitances in the above lines. Assuming $h_1 = h_2$, the line sections with subscript 2 can be approximated as symmetric stripline sections whose center conductors are at the middle between two ground planes. This kind of stripline section can be equated to a pair of ideal parallel-plate lines having an equivalent width D as shown in Fig. 17. The equivalent width D is determined as follows:

$$Y_{2o,e} = \frac{\sqrt{\epsilon_r} C_{2o,e}}{120\pi}$$

$$Y_{po,e} = \frac{\sqrt{\epsilon_r} D}{60\pi h_1}.$$

Let

$$Y_{2o,e} = Y_{po,e}$$

we obtain

$$D = \frac{C_{2o,e}}{2} h_1.$$

The line sections with subscript 1 are treated in a similar way, employing the equivalence given in Fig. 18. Assuming that the ideal parallel-plate line sections have the same equivalent width D as the line sections with subscript 2, we see that the height of the lower parallel-plate line is still equal to h_1, but the height of the upper parallel-plate line is h_0 instead of $(h_2 + h_3)$, where h_0 can be determined by making the capacitance $(C_{1o,e} - C_{2o,e}/2)$ of the upper part of the stripline equal to the capacitance D/h_0 of the upper ideal parallel-plate line

$$h_0 = \frac{C_{1o,e} - C_{2o,e/2}}{D}.$$

Since the discontinuity between the two kinds of striplines with subscript 1 and 2 is only present in the upper parts of the striplines, the corresponding discontinuity capacitances $C_{1o,e}$ may be derived in terms of upper equivalent parallel-plate lines with heights h_0 and h_2. Referring to Fig. 19 and 18, the admittance $Y^u_{1o,e}$ on the left side in Fig. 19 becomes

$$Y^u_{1o,e} \simeq \frac{\sqrt{\epsilon_r}(C_{1o,e} - C_{2o,e}/2)}{120\pi}.$$

The difference Δh_0 of the heights for both sides is

$$\Delta h_0 = h_0 - h_1 = \frac{C_2 - C_1}{C_1 - C_2/2} h_1. \tag{B2}$$

Substituting (B2) into (25b), we obtain

$$y_{o,e} = \frac{\Delta h_0}{2h_0} = \frac{C_2 - C_1}{C_2}. \tag{B3}$$

Actually, (B3) is exactly the same as (31) if we substitute (32) into (31). Finally, making use of (25), we find the discontinuity capcitances $C_{do,e}$.

References

[1] B. J. Rubin, "The propagation characteristics of signal lines in a mesh-plane environment," *IEEE Trans. Microwave Theory Tech.*, vol. MTT-32, pp. 522–531, May 1984.

[2] C. W. Barnes, "On the impulse response of a coupled-mode system," *IEEE Trans. Microwave Theory Tech.*, vol. MTT-13, pp. 432–435, 1965.

[3] S. D. Malaviya and V. P. Singh, "Transmission lines loaded at regular intervals," *IEEE Trans. Microwave Theory Tech.*, vol. MTT-27, pp. 854–859, Oct. 1979.

[4] K. K. Li, G. Arjavalingam, A. Dienes, and J. R. Whinnery, "Propagation picosecond pulses on microwave striplines," *IEEE Trans. Microwave Theory Tech.*, vol MTT-30, pp. 1271–1273, Aug. 1982.

[5] Q. Gu and J. A. Kong, "The impulse response of a non-uniformly coupled transmission line system," *J. Electromagnetic Waves and Applications*, 1986.

[6] W. J. Getsinger, "Analysis of certain transmission-line networks in the time domain," *IRE Trans. Microwave Theory Tech.*, vol MTT-8, pp. 301–309, May 1960.

[7] A. Feller, H. R. Kaupp, and J. J. Digiacomo, "Crosstalk and reflections in high-speed digital systems," in *Proc. Fall Joint Computer Conf.*, 1965, pp. 511–525.

[8] G. F. Ross, "The transient analysis of certain TEM mode four-port networks," *IEEE Trans. Microwave Theory Tech.*, vol. MTT-14, pp. 528–542, Nov. 1966.

[9] F. Y. Chang, "Transient analysis of lossless coupled transmission lines in a nonhomogeneous dielectric medium," *IEEE Trans. Microwave Theory Tech.*, vol. MTT-18, pp. 616–626, Sept. 1970.

[10] J. Chilo and T. Arnaud, "Coupling effects in the time domain for a interconnecting bus in high-speed GaAs logic circuits," *IEEE Trans. Electron Devices*, vol. ED-31, pp. 346–352, Mar. 1984.

[11] N. Yoshida and J. Fukai, "Transient analysis of a stripline having a corner in three-dimensional space," *IEEE Trans. Microwave Theory Tech.*, vol. MTT-32, pp. 491–498, May 1984.

[12] W. T. Weeks, "Calculation of coefficient of capacitance of multiconductor transmission lines in the presence of a dielectric interface," *IEEE Trans. Microwave Theory Tech.*, vol. MTT-18, pp. 35–43, Jan. 1970.

[13] E. K. Kuester and D. C. Chang, "Closed-form expressions for the current or charge distribution on parallel strips or microstrips," *IEEE Trans. Microwave Theory Tech.*, vol. MTT-28, pp. 254–259, Mar. 1980.

[14] R. E. Collin, *Field Theory of Guided Waves*. New York: McGraw-Hill, 1960.

[15] A. A. Oliner, "Equivalent circuits for discontinuities in balanced strip transmission line," *IEEE Trans. Microwave Theory Tech.*, vol. MTT-3, pp. 134–143, 1955.

[16] E. G. Cristal, "Coupled-transmissional-line directional couplers with coupled lines of unequal characteristic impendances," *IEEE Trans. Microwave Theory Tech.*, vol. MTT-14, pp. 377–346, July 1966.

Qizheng Gu was born in Jiangsu China, He graduated from Fudan University, Shanghai, China in 1960.

From 1960 to 1962, he worked on the design and analysis of automatic control systems at Shanghai Designing Institute of Machinary and Electrical Engineering, China. In 1962, he joined the Department for Research and Development at Shanghai Xinhua Radio Factory, where he was engaged in research of microwave passive and active devices, receiver systems, PLL and AFC systems, and microwave integrated circuits. Since October 1982, he has been a Senior Engineer and the Deputy Director of the Department for Research and Development. In June 1983, he came to the United States as a Visiting Scientist in the Research Laboratory of Electronics, Massachusetts Institute of Technology. His research is on electromagnetic transmission and interference in high-speed microelectronic integrated circuits.

Mr. Gu is a member of Shanghai Electronics Association Council and the Microwave Committee of the Chinese Institute of Electronics.

Jin Au Kong (S'65–M'69–SM'74–F'85) is a Professor of Electrical Engineering at the Massachusetts Institute of Technology in Cambridge, Massachusetts. Since 1984, he has been Chairman of Area IV on Energy and Electromagnetic Systems. From 1977 to 1980, he served the United Nations as a High-Level Consultant to the Under-Secretary-General on Science Technology, and as an Interregional Advisor on remote sensing technology for the Department of Technical Cooperation for Development. He has been a consultant to many government and private organizations including the Raytheon Company, the Hughes Aircraft Company, Schlumberger-Doll Research, and the MIT Lincoln Laboratory. He was also an External Examiner for the Electronics Department of the Chinese University of Hong Kong (1981–83), and an IEEE Antennas and Propagation Society Distinguished Lecturer (1982–84). In 1985, he received the excellence in teaching award from the graduate student council at MIT.

His research interest is in the area of electromagnetic wave theory and applications. He has published five books, over 120 refereed journal articles, and 80 conference papers, and supervised over 70 theses. He is the author of *Electromagnetic Wave Theory*, the editor of the Wiley series in remote sensing, and the Editor-in-Chief of the *Journal of Electromagnetic Waves and Applications*.